

# The Dynamic Response of a Weapon's Internal Components to a High Speed Impact<sup>1</sup>

Jeffrey D. Gruda  
Material & Structural Mechanics Department  
Sandia National Laboratories  
Albuquerque, New Mexico 87185-0437

The dynamic response of a weapon's internal components to an accident is critical in determining the safety of a weapon. The primary objective of this study was to determine the safety of the weapon based on the acceleration histories of its safety components. The accident scenario was a 80 feet/second impact of the weapon onto a railroad rail. Large deformations and many contacts were expected due to the severity of the impact condition. The complexity of this analysis required a nonlinear finite element code which could track many contact surfaces simultaneously and simulate material failure using element death. The damage to the structure and its contents was simulated using PRONTO3D (an explicit finite element code developed at Sandia National Laboratories). Some of PRONTO3D's advanced features used in the calculations included the self-contacting algorithms, material death, and rigid body mechanics. Throughout the analysis, a large number of mechanical contacts, both normal and sliding with friction, were detected and tracked by PRONTO3D. The analysis predicted large deformations and material failure that took the form of tears in the aluminum shroud and in the housing of the components. The predicted acceleration histories were then used to determine if the components remained functional.

## DISCLAIMER

This report was prepared as an account of work sponsored by an agency of the United States Government. Neither the United States Government nor any agency thereof, nor any of their employees, makes any warranty, express or implied, or assumes any legal liability or responsibility for the accuracy, completeness, or usefulness of any information, apparatus, product, or process disclosed, or represents that its use would not infringe privately owned rights. Reference herein to any specific commercial product, process, or service by trade name, trademark, manufacturer, or otherwise does not necessarily constitute or imply its endorsement, recommendation, or favoring by the United States Government or any agency thereof. The views and opinions of authors expressed herein do not necessarily state or reflect those of the United States Government or any agency thereof.

# MASTER

1. This work was performed at Sandia National Laboratories and supported by the U. S. Department of Energy under contract DE-AC04-94AL85000.

DISTRIBUTION OF THIS DOCUMENT IS UNLIMITED

LW/MTG

RECEIVED

FEB 14 1995

O.S.T.I.

## **DISCLAIMER**

**Portions of this document may be illegible in electronic image products. Images are produced from the best available original document.**

## 1.0 Introduction

As part of a study of a Sandia nuclear weapon, detailed structural analyses were used as an aide to determine the safety of the weapon based on the survivability of its safety components in an accident. The accident scenario analyzed was one in which the weapon impacts a railroad rail side-on at 80 feet/second. The components of the weapon were modelled to determine their acceleration histories caused by the impact. The operation of the components is based on two threshold values, peak acceleration and velocity change. Both of the values have to be exceeded for the component to be considered non-functional. Using the analysis results, a determination was made about the safety of the weapon based on the acceleration histories of the components.

The finite element calculations were done using PRONTO3D [1] which is an explicit finite element code developed at Sandia National Laboratories. Many of PRONTO3D's advanced capabilities were used in the safety calculations. Some of the capabilities used included the self-contacting detection, material death and rigid body mechanics.

## 2.0 Methodology

### 2.1 Model Definition

The detailed finite element model of a Sandia weapon with its shipping supports attached is shown in Figure 1. The model consists of 28,631 hex and shell elements and was generated using PATRAN [1]. The detailed model was used to obtain acceleration histories for components in the fireset assembly (FSA). The FSA components included were the fireset (FRS), the trigger switch (TS), the intent strong link (ISL), and the environmental sensing

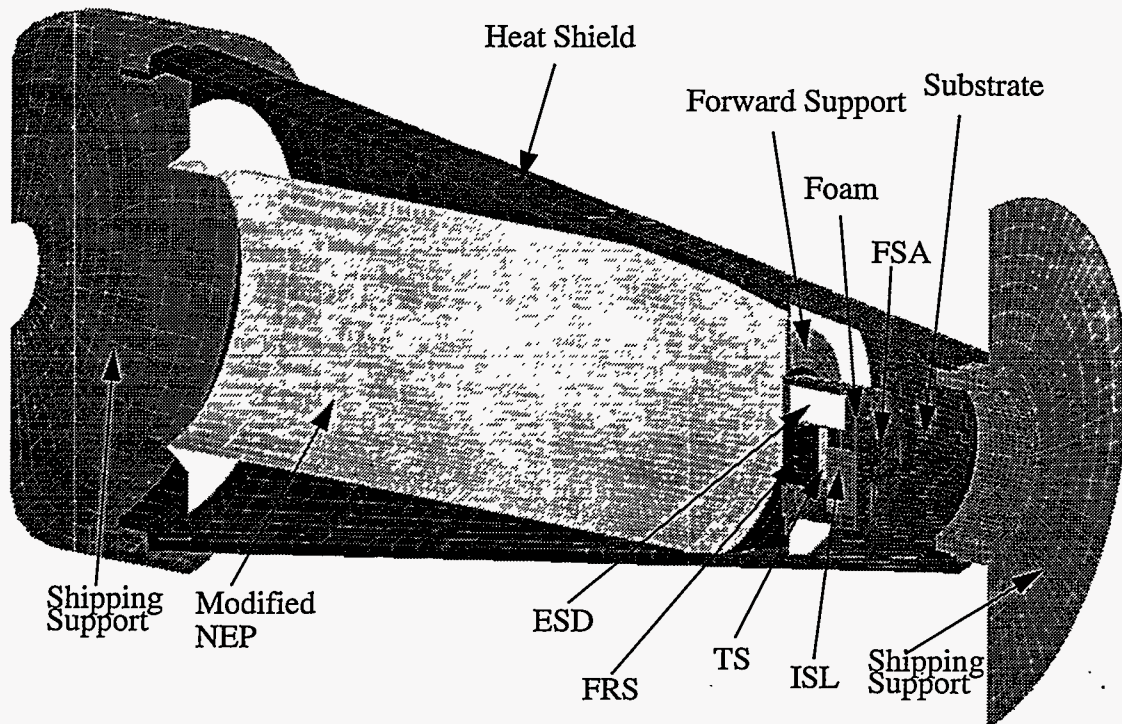


*Figure 1.* Detailed finite element model of a Sandia weapon.

device (ESD).

There are 15 major structural components in the finite element model. Table 1 lists each component, its material, and its material model used in the finite element calculations. The listing of a pseudo-material indicates that the density of the material was modified to obtain the correct weight since the geometry of the component may have been slightly modified. The only structure modelled as a rigid body was the nuclear explosives package (NEP).

As mentioned above, the finite element calculations were performed using PRONTO3D. The capabilities of PRONTO3D used to perform these simulations were element death, rigid body dynamics, point masses and inertias, and contact algorithms. The element death capability was used to model the tearing, perforation, and erosion of a material. Death limits are a user-defined criterion that enables PRONTO3D to remove an element once a predefined threshold is exceeded. These values include effective plastic strain, von Mises stress and many others. In each of the five accident scenarios, the death option was applied to the heat shield, the substrate, the FSA bolts, and the FSA container and baseplate. The rigid body option was used to model the NEP, and a point mass and point inertia were used to complete the NEP's mass properties since the exact geometry was not modelled.

## 2.2 Assumptions and Approximations

One major assumption made when modelling the weapon is that a vertical plane of symmetry exists along the axis of the weapon (see Figure 1). The FSA components were slightly

**Table 1:** Major structural components, their materials, and material model.

|    | <b>Structural Component</b> | <b>Material</b>       | <b>Material Model</b> |
|----|-----------------------------|-----------------------|-----------------------|
| 1  | Substrate                   | Aluminum 7049         | Elastic-Plastic       |
| 2  | Forward Support             | Titanium              | Elastic-Plastic       |
| 3  | FSA Baseplate               | Pseudo-Material       | Elastic-Plastic       |
| 4  | Fireset                     | Pseudo-Material       | Elastic               |
| 5  | Trigger                     | Pseudo-Material       | Elastic               |
| 6  | FSA Internal Barrier        | 304L Stainless Steel  | Elastic-Plastic       |
| 7  | Switch                      | Pseudo-Material       | Elastic               |
| 8  | ESD                         | Pseudo-Material       | Elastic               |
| 9  | FSA Container               | Pseudo-Material       | Elastic-Plastic       |
| 10 | Modified NEP                | Pseudo-Material       | Rigid                 |
| 11 | Heat Shield                 | Carbon Phenolic       | Elastic-Plastic       |
| 12 | Shipping Supports           | 304L Stainless Steel  | Elastic               |
| 13 | Foam                        | 15 lb/in <sup>3</sup> | Orthotropic Crush     |
| 14 | Rail/Flat PLate             | Mild Steel            | Elastic               |
| 15 | Bolts                       | AMS 5732              | Elastic-Plastic       |

modified to make them symmetric along this plane assuming that the modifications would not significantly change the results. Another assumption used in the analyses is that the NEP could be modelled as a rigid body. The NEP was represented as a rigid body since no large deformations would occur in the region of the NEP, and that there would not be contact between the NEP and the rail for a given accident scenario. The geometry of the NEP was simplified to a cylindrical shape since the exact geometry was not needed to detect contact; however, the mass properties of the NEP were modelled using a point mass and point inertia. Also, the components were treated as elastic bodies; thus, component plastic deformations were not calculated but acceleration histories could be recorded at the center of gravity.

The behavior of the connection between the FSA and forward support is primarily dictated by the response of the bolts. PRONTO3D is capable of accurately modelling this interaction, but the connection was simplified for the following reasons. First, knowledge about the type of failure was not known since no experimental data existed. This information would have given insight into the proper modelling technique for this region. It would have helped to have known about both the material response (ductile or brittle failure) of the bolts and their failure mode (shear, tensile, or pull-through). Second, detailed modelling of the bolts would have caused the time step of the calculation to become prohibitively small. Thirdly, the speed of the impact was expected to deliver forces which would overwhelm the eight small bolts used to secure the FSA to the forward support. Therefore, the behavior of each bolt was approximated using a single hex element.

Tearing in the substrate was simulated by constructing a ductile failure material model using experimental data on aluminum 7049 [3, 4]. The death option was then applied to a tearing parameter in the material model. The death option in PRONTO3D was used to simulate failure in many of the materials. For all of the calculations, death was applied to the following values of effective plastic strain: 5% for carbon phenolic, 15% for titanium, approximately 30% for NOAH, and 22% for the bolts [5].

### **3.0 Results**

For the rail impact analysis, the following will be presented: 1) undeformed model, 2) deformed model of the FSA region, 3) acceleration history plots of the FSA, TS, ISL, and ESD, 4) and comments on bolt survivability.

#### **3.1 Case 1**

In this accident scenario, the warhead impacted a railroad rail side-on at 80 feet/second. The finite element model is shown in Figure 2, and Figure 3 shows the deformed model at 4.0 ms. The deformed mesh shows that there were tears in the substrate and a hole in the heat shield. Although it cannot be seen from this view, there was also a hole in the container of the FSA. The bolts that hold the FSA to the forward support failed and the entire FSA was significantly displaced. The kinetic energy used in this calculation was 16.1% of its initial value, and 5.1% was consumed penetrating through the heat shield and substrate to the outer edge of the FSA. The peak component accelerations occurred when the rail impacted the FSA. The acceleration history of each component is shown in Figure 4. No filtering was applied except for the output frequency of the finite element code. A summary of the peak accelerations and velocity changes for each of the components is listed in Table 2.

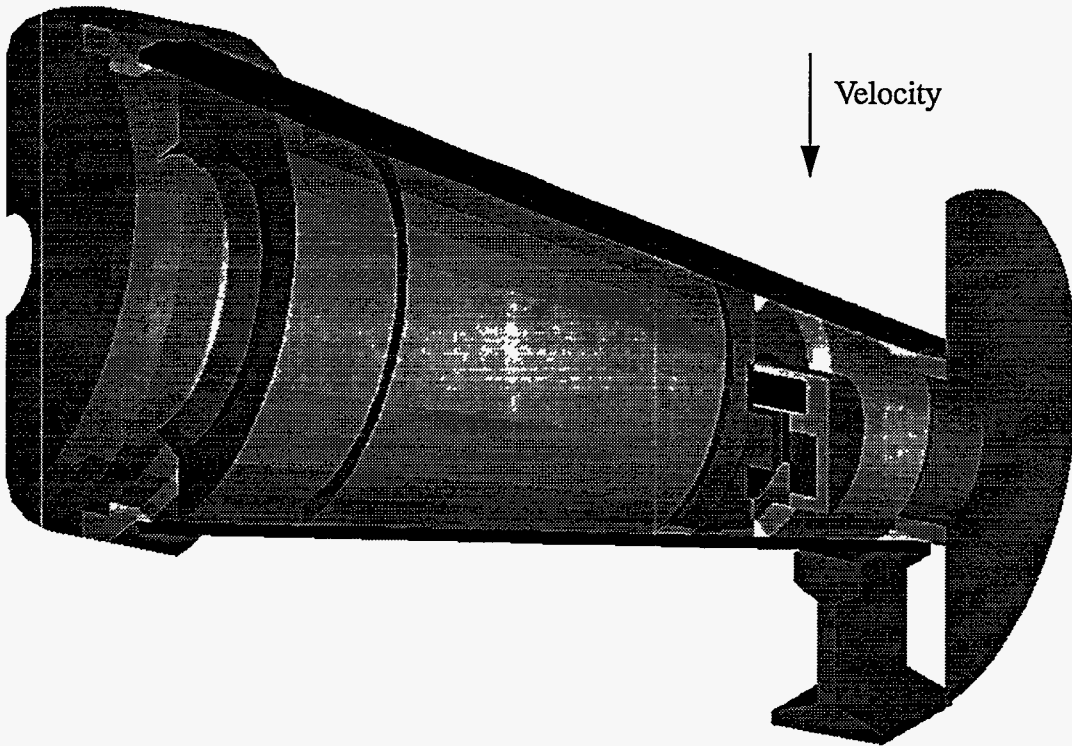


*Figure 2.* Initial setup of the rail-weapon impact at 80 feet/second.

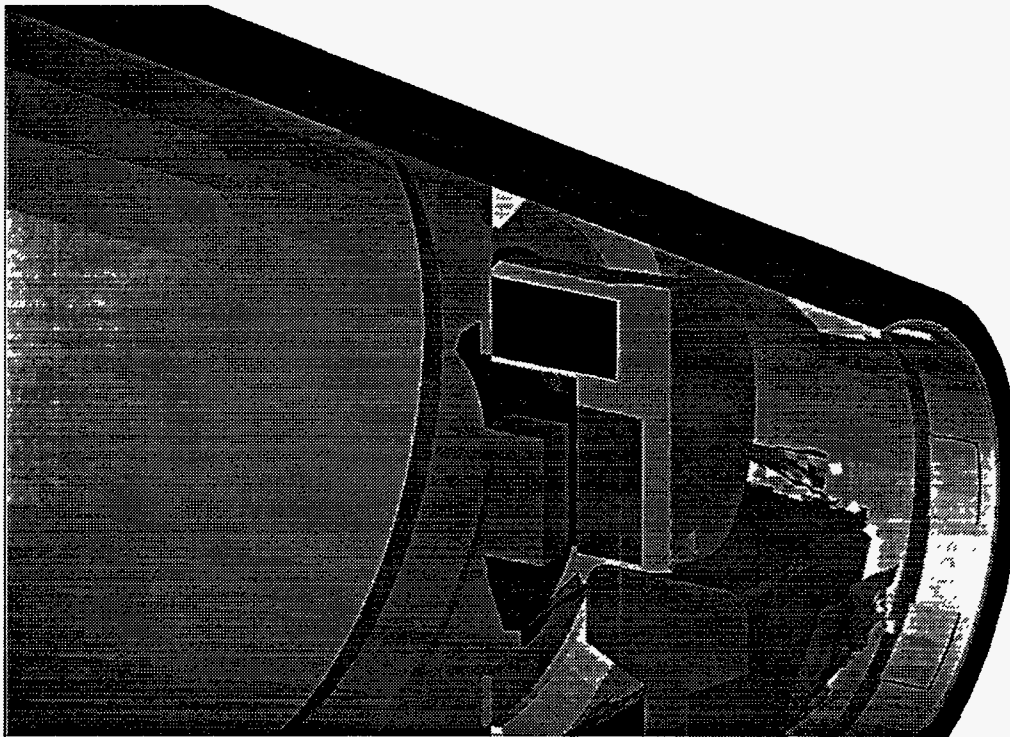


*Figure 3.* Deformed shape of Case 1 at 4.0 ms.

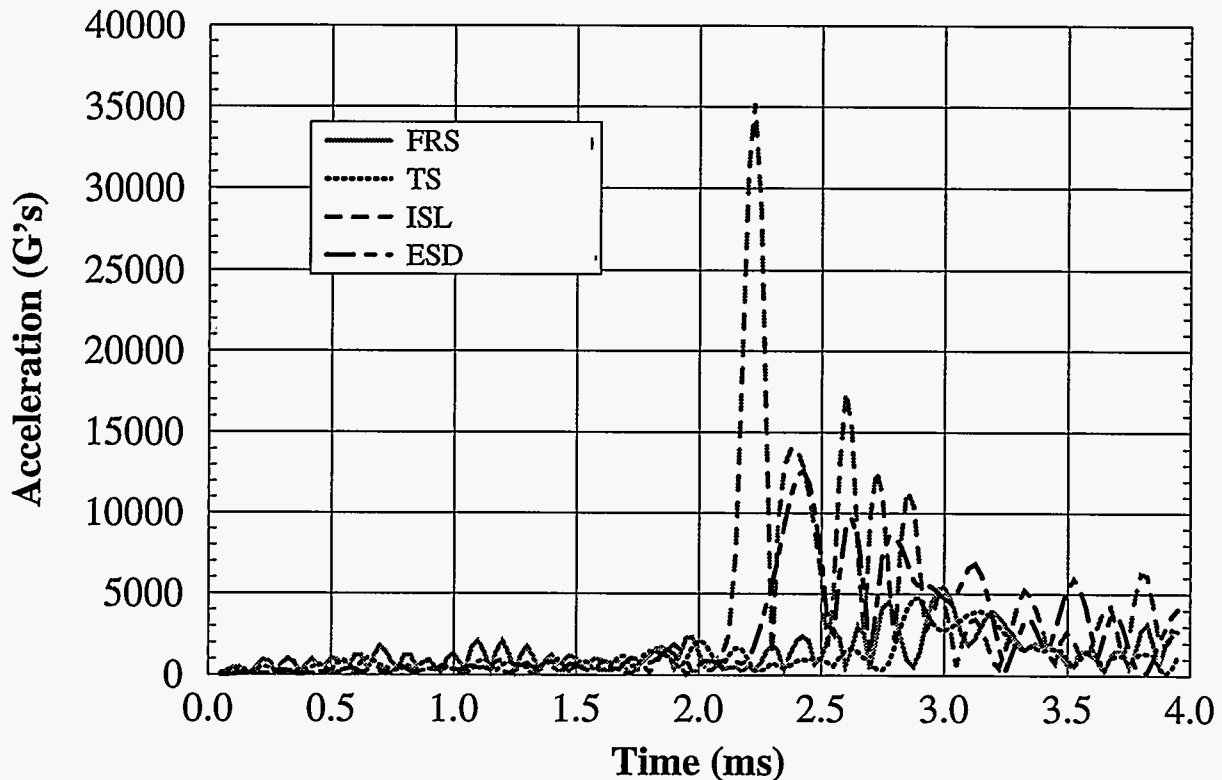


Figure 4. Component acceleration histories for Case 1.

### 3.2 Case 2

The analysis of Case 2 is similar in impact speed and orientation to Case 1 except that the substrate was removed from the forward support toward the front of the weapon, and the heat shield was removed in addition to the forward shipping support. This model consisted of 15,250 hex and shell elements. Figure 5 shows the model in its initial condition, and Figure 6 shows the deformed shape at 2.35 ms. The analysis of Case 2 was used to determine the difference the heat shield and substrate made on the loading of the components. Figure 7 shows the acceleration histories of the components. Table 2 is a summary of peak G levels and velocity changes that each component experienced for Cases 1 and 2. Comparing these cases shows that the components directly in line with rail (ISL and ESD) show little difference in both peak acceleration and velocity change. On the other hand, the FRS and TS have significant differences. This is due to the load path taken through the substrate and then into the baseplate of the FSA. In Case 2 the loading in the components is not seen until the rail impacts the FSA. Only 6.1% of the initial kinetic energy was used to displace the FSA the same distance as in Case 1. Through this large displacement, the FSA bolts did fail.

Table 2: Summary of component peak G levels and velocity changes for a rail impact.

| Case | FRS   |       | TS   |       | ISL    |       | ESD    |       |
|------|-------|-------|------|-------|--------|-------|--------|-------|
|      | G's   | G-sec | G's  | G-sec | G's    | G-sec | G's    | G-sec |
| 1    | 4,800 | 2.54  | 3300 | 3.04  | 26,100 | 3.24  | 11,600 | 2.37  |
| 2    | 3,300 | 1.45  | 4200 | 2.31  | 26,700 | 3.43  | 12,900 | 2.59  |

Figure 6. Deformed shape of Case 2 at 2.35 ms.

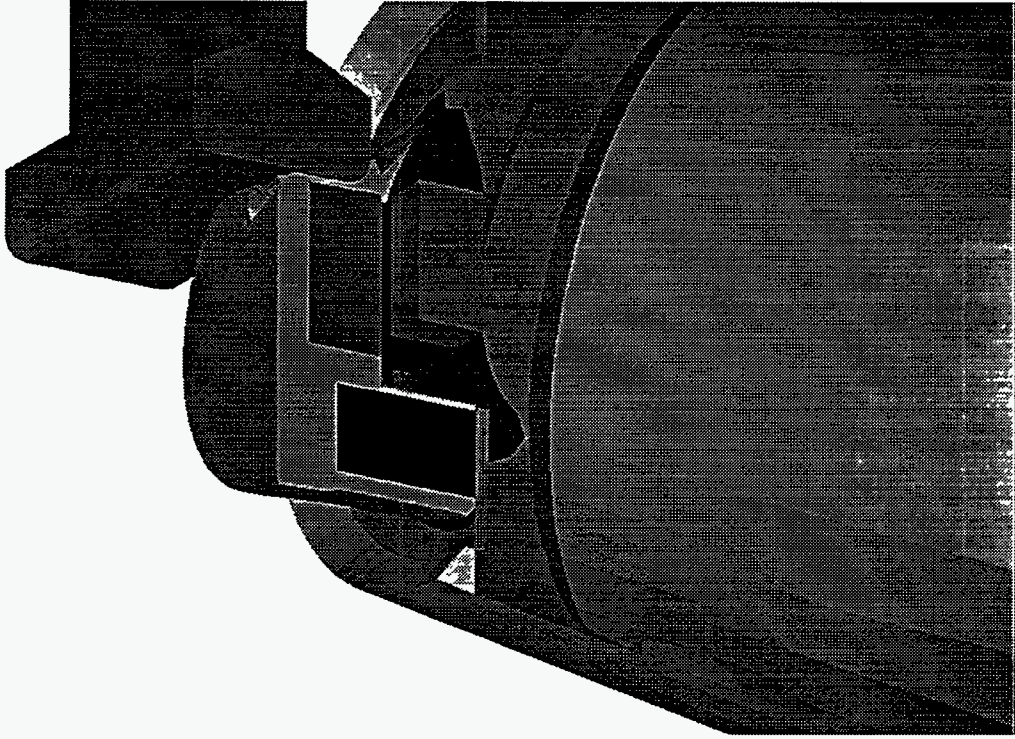
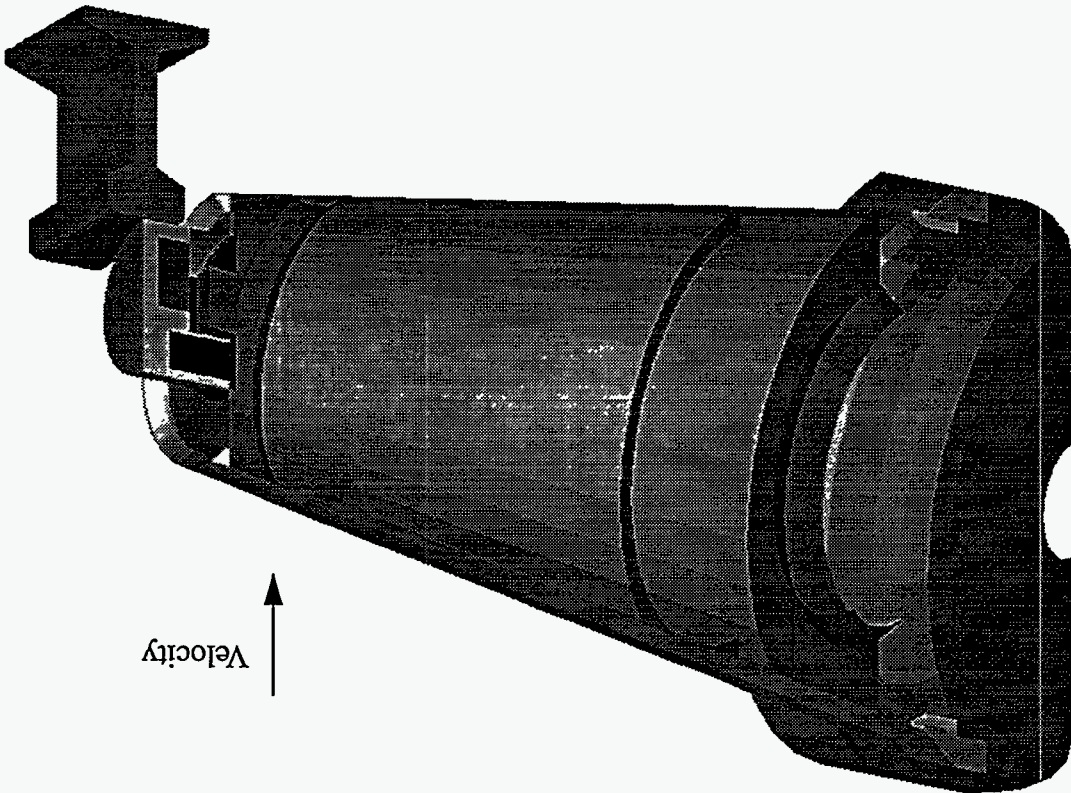


Figure 5. Initial setup of Case 2.





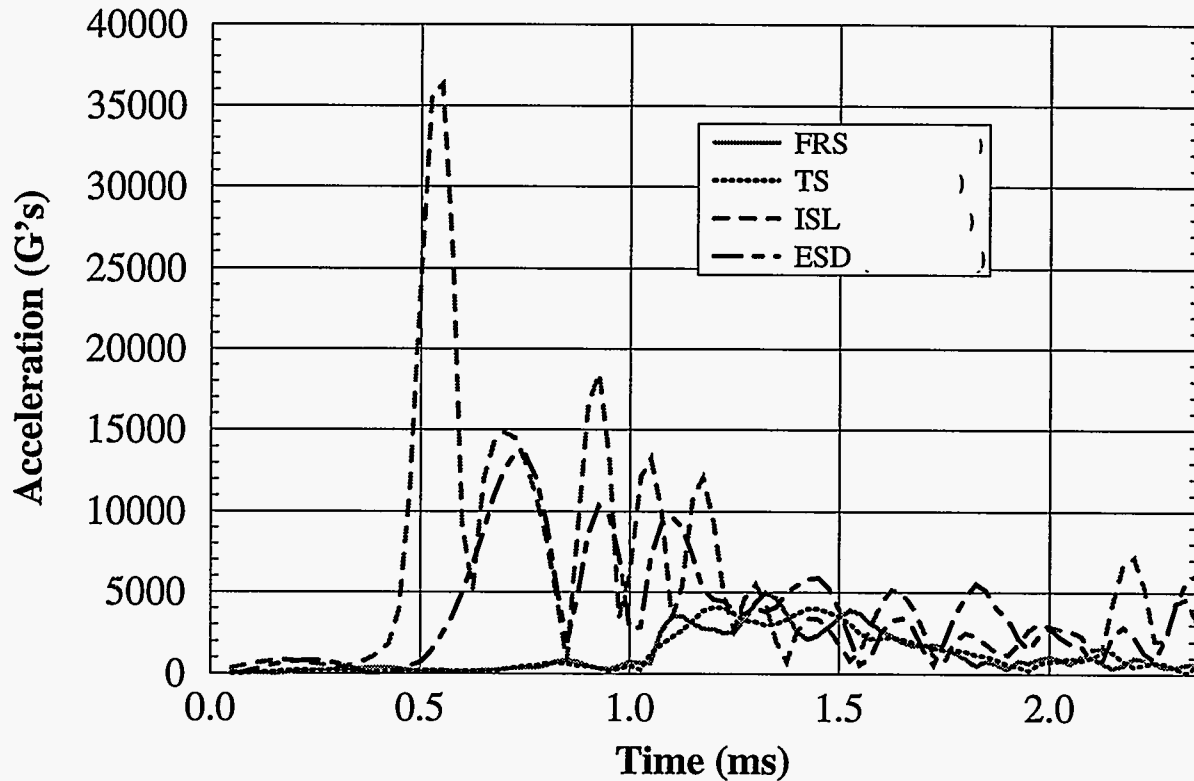


Figure 7. Component acceleration histories for Case 2.

#### 4.0 Conclusions

The results of the analyses show that the velocity was high enough to cause the FSA bolts to fail. The results also show that components being directly hit by the rail have similar peak accelerations with or without the heat shield and substrate. These components include the ISL and ESD. The peak accelerations of the FRS and TS are dependent on the load path to the FSA. However, the cost savings of the PRONTO3D calculation is considerable with the smaller finite element model. For example, the cost and cpu times needed to analyze Case 2 is 1/5 that of Case 1. The size of the model in Case 2 is approximately half the size of that in Case 1. Finally, the results of the analyses have not been compared to experimental data. To develop an accurate model, experimental data are needed.

## 5.0 References

1. PATRAN Plus User's Manual, Volumes I and II, Release 2.4.
2. Taylor, L. M. and Flanagan, D. P., "PRONTO3D - A Three-Dimensional Transient Solid Dynamics Program," SAND86-0594, Sandia National Laboratories, 1987.
3. Crenshaw, T., "Tensile Testing of 7049 Aluminum," Memo to J. D. Gruda, Sandia National Laboratories, August 11, 1993.
4. Stone, C. M. and Wellman, G. W., "Implementation of Ductile Failure in PRONTO2D and PRONTO3D," Memo to Distribution, Sandia National Laboratories, April 8, 1993.
5. Military Handbook, "Metallic Materials and Elements for Aerospace Vehicle Structures," Department of Defense, Volumes I and II, MIL-HDBK-5E, June 1, 1987.